



Synthesis, Molecular Modeling and QSAR Studies in Chiral 2,3-disubstituted-1,2,3,4-tetrahydro-9H-pyrido(3,4-b)indoles as Potential Modulators of Opioid Antinociception[†]

Anil K. Saxena,^{a,*} Suresh K. Pandey,^a Ravish C. Tripathi^a and Ram Raghubir^b

^aDivision of Medicinal Chemistry, Central Drug Research Institute, Lucknow 226001, India

^bDivision of Pharmacology, Central Drug Research Institute, Lucknow 226001, India

Received 16 October 2000; accepted 31 January 2001

Abstract—In view of coexistence of opioid and cholecystokinin (CCK) in the brain areas concerned with pain processing, some semirigid racemic and chiral analogues of a potent CCK receptor antagonist (*benzotript*) have been synthesized and tested for their modulatory role on opioid antinociception, which may be mediated by CCK-B receptor. Some of these compounds, **3e**, **3g**, **3h**, **4a**, **4b** and **4h**, exhibited antinociceptive potentiation comparable to *benzotript* and *proglumide*. In order to identify the essential chemical structural features important for this potentiation, molecular modeling and quantitative structure activity relationship (QSAR) studies have been carried out in the *S* and *R* enantiomers of some of these semi-rigid compounds. The 3D-biophore models, common to all molecules of the training set have been derived. These models with superimposition (match value >0.25) depicted three biophoric sites one each for, π /hydrophobic interactions, hydrogen bonding and ionic interactions among the phenyl/pyrrole ring, indole nitrogen, amidic oxygen, pyridyl nitrogen and lone pair of amidic oxygen. The total hydrophobicity and *S* absolute stereochemistry are found to positively contribute to potentiation of antinociception induced by morphine and the resulting quantitative pharmacophoric model with good correlation is found to well describe the observed activity. © 2001 Elsevier Science Ltd. All rights reserved.

Introduction

Despite several analgesics, the opioids still remain the main drug of choice for the relief of the pain in humans and morphine is still a drug of choice in such situations. There is a high patient-to-patient variability in response to opioids¹ and complete pain control is only achieved by increasing the dose, which causes side effects like nausea, respiratory depression and mood disturbance. This is further complicated by the other major drawback of tolerance development² to the analgesic effect (of opioid/morphine). Therefore, the efforts have been to develop adjuvant drugs, which can potentiate the analgesic effect of morphine/opioids and at the same time counteract their abuse potential.

Several strategies to block the opioid tolerance include NMDA antagonists and nitric oxide synthase inhibitors, which have been shown to attenuate the tolerance

development to morphine in rodents;^{3–6} however, their clinical use in the pain management as adjuvants is limited due to their own adverse side effects.⁷

The 5-HT receptor antagonists have been shown to inhibit the expression of tolerance,^{8–10} the inter-connection of opioid and serotonergic systems in the circuitry underlying nociceptive neurotransmission in the CNS.^{11–13} However, the precise role of the serotonergic system in the tolerance process is still not well explained.⁸

In view of the coexistence of opioid and cholecystokinin (CCK) in the brain areas concerned with pain, processing indicates neuromodulatory role of CCK in opioid antinociception. The observations that exogenous cholecystokinin selectively antagonizes opiate analgesia and endogenous cholecystokinin system opposes the action of opiates, the CCK receptors have been implicated in the attenuation of morphine-induced antinociception.^{14,15} CCK is a polypeptide consisting of 33-amino acid and is distributed in various molecular forms in the central nervous system (CNS) as well as in the peripheral tissues. The biological actions of CCK are manifested by two receptor subtypes, CCK-A (alimentary) and CCK-B

[†]CDRI Commun. No. 6054. Part of the work has been presented in the Vth IUPAC International Symposium on Bio-organic Chemistry (ISBOC 5), 30 January–4 February 2000 at NCL, Pune.

*Corresponding author. Tel.: +91-522-212411-18, extn. 4268; fax: +91-522-223405/223938/229504; e-mail: anilsak@hotmail.com

(brain), both of which have been cloned and their expression is now known.^{16–18} The CCK-A receptor is predominantly found in peripheral tissues such as the pancreas, colon, and gallbladder, although low levels of this subtype are also found in discrete regions of the CNS.¹⁹ The CCK-B receptor is primarily located in the CNS and is indistinguishable from peripheral gastrin receptors on the basis of both their binding properties²⁰ and comparison of the amino acid sequences deduced from cloned receptor cDNA of brain and gastric mucosa.²¹ The coexistence and interaction of CCK-B with other neurotransmitters, for example, dopamine, GABA^{22,23} and neuropeptides, for example, neurotensin and substance P,²⁴ support involvement of CCK-B in variety of neurological disorders such as anxiety, pain and panic disorder.^{25,26}

CCK receptor antagonists could be broadly classified into the four classes: (1) derivatives of cyclic nucleotides, (2) partial sequences of the C-terminal region of CCK, (3) derivatives of amino acids, for example, *proglumide*, *benzotript*²⁷ and its analogues, (4) benzodiazepine derivatives. As *benzotript* is a flexible molecule, it may have many possible conformations. Out of them, only certain discrete conformations may be responsible for the specific biological activity. In view of this, some semirigid racemic analogues of *benzotript* were synthesized which showed potent anti-ulcer activity comparable with *benzotript* in our earlier work.²⁸

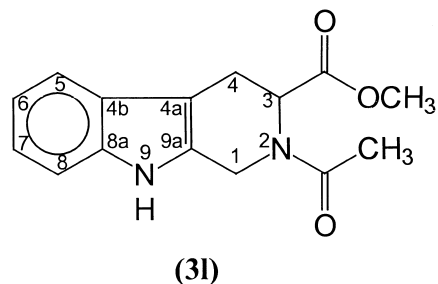
Some of the analogues, which did not show significant anti-ulcer activity, showed potentiation of morphine antinociception, which may be mediated by CCK-B receptor. Thus, there was a need to identify the essential chemical structural features important for this activity for which the *S* and *R* enantiomers of some of these semi-rigid compounds were synthesized, evaluated and 3D-QSAR study undertaken. Such QSAR's are a useful tool in the medicinal chemistry in defining the forces governing the pharmacological activity of a particular class of compounds. Particularly in cases where the crystallographic structure of the pharmacological target is unknown, it is possible to use molecular modeling techniques to construct models of the receptor sites or a graphical pharmacophore²⁹ which may be used to improve description and prediction of activity. Among such approaches, hydrophobic interactions between molecules (HINT),³⁰ distance geometry,^{30,31} receptor modeling based on the three-dimensional structure and physicochemical properties of the ligand molecules (REMOTEDISC),^{32,33} hypothetical active site lattice (HASL),^{30,34} comparative molecular field analysis (CoMFA)³⁰ and the Apex-3D expert system based on the logicostructural³⁵ program are used. Apex-3D identifies biophores, which represents a certain structural and electronic pattern in a bioactive molecule, which is responsible for the manifestation of activity possible due to receptor interaction. Descriptor centers of biophores can be atoms, pseudo atoms, ring centers, hydrophobic regions and hydrogen bonding sites that can participate in ligand–receptor interactions. These descriptor centers are based on certain physical properties such as electrostatic interaction, charges, electron acceptor or donor,

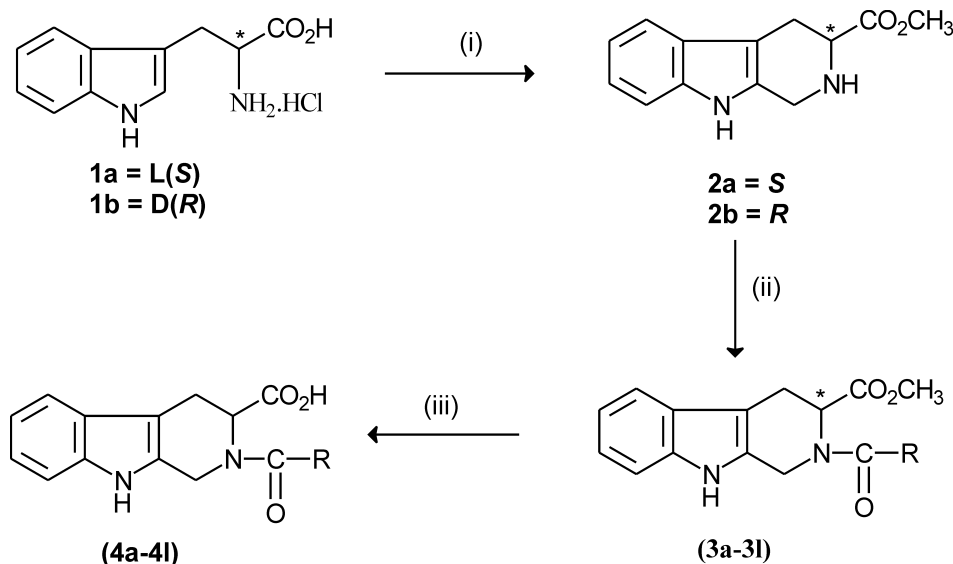
hydrogen bonds (presence), charge–transfer complexes (HOMO, LUMO), hydrophobic interactions, van der Waals (London) dispersion forces (π electron density on atoms), as well as atomic contributions to hydrophobicity and molar refractivity. This program compares the descriptors and their distances with respect to active and inactive analogues and stores the results as rules in a knowledge base, which can be used to predict the activities of novel compounds.

So the 3D-QSAR models based on common biophores have been derived on total set of 13 compounds (11 chiral title esters, *benzotript* and *proglumide*) and the models have been used to compare the observed activity of the partially racemized acids with the predicted activity of the corresponding chiral acids and results produced are reported in this paper.

Chemistry

The key intermediates *S* and *R* methyl 1,2,3,4-tetrahydro-9H-pyrido(3,4-b)indole-3-carboxylate (**2a** and **2b**) were synthesized essentially according to literature method³⁶ starting from *S* and *R* tryptophan methyl ester hydrochloride (**1a** and **1b**) by Pictet Spengler cyclization of the corresponding imines obtained by condensation with formaldehyde, followed by the basification of the ester hydrochloride. These esters (**2a** and **2b**) on condensation with different acid chlorides yielded the corresponding amides **3a–3l** (Scheme 1, Table 1). Selective hydrolysis of **3a–3k** with NaOH afforded the partially racemic title acids **4a–4k** (Scheme 1, Table 1). These amidic esters **3a–3l** were chirally pure and their enantiomeric excess (ee) was >95% as was determined on chiral stationary phase column, chiraDex[®] by analytical HPLC, LaChrom of Merck. The compounds **3a–3l** had reasonable value of optical rotation almost of similar magnitude for both C-3 (*S*) and C-3 (*R*) enantiomers. However, in general, ¹H NMR spectrum of these amidic esters **3a–3l** showed two sets of signal for each proton in variable ratios depending on the steric bulk of the amidic group possibly due to the restricted rotation around an amide N–CO bond resulting in the existence of two conformers in solution state at room temperature. In order to confirm this, the ¹H and ¹³C NMR studies were carried out on relatively simple compound *S*(–)-methyl 2-acetyl-1,2,3,4-tetrahydro-9H-pyrido(3,4-b)indole-3-carboxylate (**3l**), which was prepared by the acetylation of the C-3 (*S*) ester **2a** with acetic anhydride.





Scheme 1. (i) (a) HCHO, MeOH, H₂O, Pictet–Spengler (PS) cyclization reaction; (b) NaHCO₃ saturated solution; (ii) RCOCl, Et₃N, THF, 30 °C–reflux; (iii) (a) 2N aq NaOH; (b) HCl.

Table 1. Characterization data of the title compounds^a

Compound no.	R	Configuration at C-3	mp (°C)	Yield (%)	$[\alpha]_D^{20}$	Concentration (g/mL) ^b	Molecular Formula
3a	4-Cl-C ₆ H ₄	S	245	52	-8.28	0.22	C ₂₀ H ₁₇ O ₃ N ₂ Cl
3b	2-Quinolylyl	S	125	60	-21.74	0.22	C ₂₃ H ₁₉ O ₃ N ₃
3c	Cyclohex-1-yl	S	149	73	+84.39	0.19	C ₂₀ H ₂₄ O ₃ N ₂
3d	2-COCH ₃ -C ₆ H ₄	S	158	35	-38.74	0.28	C ₂₂ H ₂₀ O ₄ N ₂
3e	3-F-C ₆ H ₄	S	120	71	+6.72	0.20	C ₂₀ H ₁₇ O ₃ N ₂ F
3f	4-F-CH ₂ -C ₆ H ₄	S	170	67	+43.75	0.19	C ₂₁ H ₁₉ O ₃ N ₂ F
3g	OCH ₂ -C ₆ H ₅	S	102	63	+62.90	0.23	C ₂₁ H ₂₀ O ₄ N ₂
3h	2-OCH ₃ -(CH=CH) ₂ -C ₆ H ₄	S	159	43	+11.32	0.10	C ₂₅ H ₂₄ O ₄ N ₂
3i	3-Cl-C ₆ H ₄	S	164	58	-10.52	0.11	C ₂₀ H ₁₇ O ₃ N ₂ Cl
3j	2-Quinolylyl	R	134	42	+20.16	0.12	C ₂₃ H ₁₉ O ₃ N ₃
3k	4-Cl-C ₆ H ₄	R	235	36	+7.54	0.11	C ₂₀ H ₁₇ O ₃ N ₂ Cl
3l	CH ₃	S	167	85	+143.68	0.21	C ₁₅ H ₁₆ O ₃ N ₂
4a	4-Cl-C ₆ H ₄	S	222	54	-1.91	0.22	C ₁₉ H ₁₅ O ₃ N ₂ Cl
4b	2-Quinolylyl	S	215	50	-2.22	0.23	C ₂₂ H ₁₇ O ₃ N ₂
4c	Cyclohex-1-yl	S	218	77	+3.22	0.21	C ₁₉ H ₂₂ O ₃ N
4d	2-COCH ₃ -C ₆ H ₄	S	250	40	-2.56	0.21	C ₂₁ H ₁₈ O ₄ N ₂
4e	3-F-C ₆ H ₄	S	230	51	-0.90	0.22	C ₁₉ H ₁₅ O ₃ N ₂ F
4f	4-F-CH ₂ -C ₆ H ₄	S	155	53	-2.23	0.27	C ₂₀ H ₁₇ O ₃ N ₂ F
4g	OCH ₂ -C ₆ H ₅	S	233	54	-2.94	0.24	C ₂₀ H ₁₈ O ₄ N ₂
4h	2-OCH ₃ -(CH=CH) ₂ -C ₆ H ₄	S	182	62	-1.49	0.20	C ₂₄ H ₂₂ O ₄ N ₂
4i	3-Cl-C ₆ H ₄	S	228	78	-5.93	0.12	C ₁₉ H ₁₅ O ₃ N ₂ Cl
4j	2-Quinolylyl	R	227	63	+2.96	0.12	C ₂₂ H ₁₇ O ₃ N ₃
4k	4-Cl-C ₆ H ₄	R	231	76	+2.96	0.11	C ₁₉ H ₁₅ O ₃ N ₂ Cl
4l	CH ₃	S	222	80	+6.48	0.20	C ₁₄ H ₁₄ N ₂ O ₃
5a	4-Cl-C ₆ H ₄	RS	254	52	NA ^c	NA	C ₁₉ H ₁₅ O ₃ N ₂ Cl
5b	2-Quinolylyl	RS	233	80	NA	NA	C ₂₂ H ₁₇ O ₃ N ₃
5c	3-F-C ₆ H ₄	RS	246	51	NA	NA	C ₁₉ H ₁₅ O ₃ N ₂
5d	3,5-(CH ₃) ₂ C ₆ H ₃	RS	242	54	NA	NA	C ₂₁ H ₂₀ O ₃ N ₂
5e	3,5-(OCH ₃) ₂ C ₆ H ₃	RS	152	41	NA	NA	C ₂₁ H ₂₀ O ₅ N ₂

^aSynthesis of racemic acids **5a–5e** was done as per ref 28.

^bOptical rotations of the esters **3a–3l** were taken in MeOH while of the acids **4a–4l** were taken in DMF.

^cNA, not applicable.

The compound *S*(-)-methyl 2-acetyl-1,2,3,4-tetrahydro-9H-pyrido(3,4-b)indole-3-carboxylate (**3l**) existed as two conformers, one major and the other minor. ¹H spectrum of **3l** showed two sets of signal for each proton (Table 2), namely 8.63 (ex, brs, 1H, NH, min) and 8.47 (ex, brs, 1H, NH, maj), 7.51 (t, *J*=4.8 Hz, 1H, Ar-5-H), 7.26–7.32 (m, 1H, Ar-8-H), 7.09–7.20 (m, 2H, Ar-6 and 7-H) 5.95 (d, *J*=6.2 Hz, 1H, CHCO₂CH₃, maj) and 4.94

(d, *J*=5.7 Hz, 1H, CHCO₂CH₃, min), 4.39 and 5.21 (d, *J*=16.8 and 17.1 Hz, respectively, 1H, CH₂N, min), 4.73 and 4.84 (d, *J*=15.3 Hz for both, 1H, CH₂N, maj), 3.62 (s, 3/2 H, OCH₃, min), 3.59 (s, 3/2H, OCH₃, maj), 3.06 and 3.47 (dd and d, *J*=6.3, 15.9 and 15.6 Hz, respectively, 1H, CH₂CHCO₂CH₃, maj), 3.15 and 3.54 (dd and d, *J*=5.76 and 15.6 Hz, respectively, 1H, CH₂CHCO₂CH₃, min), 2.27 (s, 3/2 H, COCH₃, maj)

Table 2. ^1H NMR spectrum of *S*-(-)-methyl 2-acetyl-1,2,3,4-tetrahydro-9H-pyrido(3,4-b)indole-3-carboxylate **31** (exists in two conformations, major and minor, depending on the bulk of *R* group)

Comformer	Major	Minor
1H	4.84 and 4.73 (d, $J=15.3$ for both, 1H)	5.21 and 4.39 (d, $J=17.1$ and 16.8, respectively, 1H)
3H	5.95 (d, $J=6.2$, 1H)	4.94 (d, $J=5.7$, 1H)
4H	3.47 and 3.06 (d and dd, $J=15.6$ and 6.3, 15.9, respectively, 1H)	3.54 and 3.15 (d and dd, $J=15.6$ and 5.76, 15.6, respectively, 1H)
5H		7.51 (t, $J=4.8$, 1H, indistinguishable)
6 and 7H		7.09–7.20 (m, 2H, indistinguishable)
8H		7.26–7.32 (m, 1H, indistinguishable)
9H	8.47 (ex, brs, 1H)	8.63 (ex, brs, 1H)
11H	2.27 (s, 3H)	2.26 (s, 3H)
13H	3.59 (s, 3H)	3.62 (s, 3H)

**Figure 1.** ^1H spectrum of **31** in CDCl_3 at different temperatures (298, 308, 318, 328 and 338 K). At 338 K, the two set of signals of COCH_3 and OCH_3 merged together due to free rotation of these groups.

and 2.26 (s, 3/2 H, COCH₃, min) and positions were ascertained by ¹H correlation spectroscopy (COSY) spectrum. The presence of two conformers was further confirmed by recording the ¹H spectra at different temperatures (at 298, 308, 318, 328 and 338 K) (Fig. 1). At normal temperature, the energy difference between two conformers is too large; therefore, in the NMR time scale both sets were observed separately. At higher temperature, the two signals of each COCH₃ and OCH₃ merged together due to free motion, but the protons of the ring were observed separately due to restricted rotation of the ring between two forms. The sets of proton of two conformers were also differentiated with the help of rotatory Overhauser effect spectroscopy (ROESY) spectrum. In ROESY spectra, COCH₃ of one conformer (minor) showed a cross-peak with H-3 proton, while in the other conformer (major), H-1 showed a cross-peak with H-5 phenyl proton. Exactly similar observations were there in ¹³C NMR spectra and complete assignment of chemical shift values for ¹H NMR of the representative title acid and ester compounds are given in the Experimental.

Results and Discussion

In initial studies, it was observed that the racemic semi-rigid cyclic analogue (**5a**) of *benzotript* was almost equiactive to *benzotript* in the modulation of anti-nociceptive potentiation similar to the case of CCK mediated anti-ulcer activity.²⁸ Among its two partially racemized (*S* and *R*) enantiomers, the enantiomer with predominant *S* chiral center (**4a**) was found to be more active and the enantiomer with predominant *R* chiral center (**4k**) was found to be less active than the racemic one (**5a**). Hence, the order of activity among the three semi-rigid analogues is partially racemized *S* (**4a**) > RS (**5a**) > partially racemized *R* (**4k**). Similar results were also observed with its racemic quinolyloxycarboxamide (**5b**) and its partially racemic *S* (**4b**) and *R* (**4k**) analogues where both **4b** and **5b** were almost equiactive to *benzotript*. In view of it, only compounds corresponding to *S* enantiomer were synthesized and studied for the modulation of anti-nociception. Among these, the compounds **3e**, **3g**, **3h** and **4h** exhibited anti-nociceptive potentiation comparable to the *benzotript* and *proglumide* in addition to the above discussed compound and the overall order of antinociceptive modulation was **3h** > **4h** > **3e** = **4b** > **3g** = **4a**.

The preliminary molecular modeling studies for all the 13 compounds (**3a–3k**, *benzotript* (*S* configuration) and *proglumide* (*S* configuration)) resulted in the development of biophore models with poor superimposition and only one model (model no. 1) showed match value >0.25 with three biophore sites common to all molecules (Table 4, Fig. 2); site A is the phenyl ring of indole part in terms of its 6π electrons presence which possibly involved in π–π interactions, site B being the amidic oxygen in terms of π population charge and the electron donating index for electrostatic as well as for ionic binding and its lone pair as third site C for hydrogen bonding. The mean value of the three properties (π-population, charge and electron donor

reactivity (Don₀₁) of site B corresponding to the amidic oxygen in the compounds (**3a–k**), *benzotript* and *proglumide* are 0.986 ± 0.027, –0.362 ± 0.029 and 8.370 ± 0.115 Å, respectively. The spatial disposition with respect to each in terms of distances between three biophoric centers A, B and C for the compounds is described as the mean values between A and B, B and C and A and C which are 7.583 ± 0.217, 3.000 ± 0.001 and 9.697 ± 0.465 Å, respectively. The similarity of these results with earlier reported molecular modeling results in case of CCK-B antagonist³⁷ points that anti-nociceptive action of title molecule is mainly due to their CCK-B antagonism and the model selected conform to the earlier suggested model of binding CCK-B antagonist to the receptor where hydrogen bond is formed between the carbonyl oxygen of the ligand and properly oriented receptor donor function and possibly hydrophobic pocket exist in the receptor cavity which offers additional sites for anchoring. The best quantitative structure–activity relationship derived for this model (model no. 1; Table 5) is shown by the two-parameter equation (eq. 1):

$$\begin{aligned} \text{Log}(C \times 100) &= 0.255 (\text{total hyd.}) - 0.628 (J) + 0.452 \\ n &= 13, R = 0.880, \text{RMSA} = 0.140, F_{2,10} = 17.224; \\ F_{2,10\alpha 2 : 0.002} &= 14.9 \end{aligned} \quad (1)$$

The equation has reasonably good correlation coefficient value ($R=0.880$) of high statistical significance >99.8% ($F_{2,10}=17.224$; $F_{2,10\alpha 2:0.002}=14.9$). The equation is also of good predictive value (R^2 cross-validated = 0.730). The positive regression coefficient with total hydrophobicity points towards the positive contribution and importance of this parameter for the potentiation of antinociception (C) in these compounds. The negative contribution of the indicator variable (J) which has value of 0 and 1 for *S* and *R* stereochemistry respectively, at C-3 center simply quantifies the positive contribution of *S* stereochemistry at this center for activity. This model (eq 1), describes well the experimentally observed activity data and the calculated as well as predicted (leave one out) activity data (Table 6). A careful comparison of this data indicates that predicted and calculated error values 0.32 and 0.25 were the highest for *proglumide* in this series of compounds. This may possibly be due to structural dissimilarity between *proglumide* and rest of the molecules. The same may also reason for the poor superimposition, that is, low match value (0.26). Hence, attention was focused to the biophore models with 12 compounds (*proglumide* excluded). Among several of these models, five models (model nos. 2–6, Fig. 3) with match value >0.35, which had three biophoric sites, were considered. As expected this set of 12 compounds showed significant improvement in the superimposition as indicated by higher match values than that of model no. 1 because of the exclusion of most dissimilar structure *proglumide*. The model no. 2 had two biophoric sites amidic oxygen and its lone pair similar to model no. 1, however it took indole nitrogen atom as third biophoric site as compared to the phenyl ring center of indole in model no.1. In model no. 3, all the three biophore sites, namely

phenyl ring center, pyrrole ring center and nitrogen of the pyrrole ring exists in indole nucleus near to each other. The two-biophore sites in model nos. 4 and 5 were the same in all respect, that is, in terms of ring center of phenyl ring and nitrogen of the pyridine ring except in model no. 5 which had third biophore site as pyrrole ring while in model no. 4 it was nitrogen atom of the indole ring. However, model no. 4 has been better in terms of match value as compared to model no. 5. Model no. 6 was not found appropriate because *benzotript*, which is a flexible molecule, so in its alignment with other molecules it used its benzene ring center at a particular biophoric site while the rest of the molecules used their amidic oxygen; however, the rest of the biophoric sites in the model were the same for the total set of molecules (Fig. 2). These biophore models (nos. 2–6) were also used to derive quantitative structure activity relationships similar to the one corresponding biophore model 1 (eq (1)) and surprisingly the best results corresponded to eq (1) and were similar for all these biophore models (eq. (2)) because it did not contain any 3D or secondary site parameters.

$$\begin{aligned} \text{Log}(C \times 100) &= 0.333 (\text{total hyd.}) - 0.617 (J) + 0.202 \\ n &= 12, R = 0.927, \text{RMSA} = 0.113, F_{2,9} = 27.636; \\ F_{2,9} \alpha_{2:0.001} &= 19.9 \end{aligned} \quad (2)$$

The comparison of the regression coefficient of both the parameter total hydrophobicity and indicator variable showed similarity both on terms of magnitude and sign. This stability of regression coefficients and the improvement in correlation coefficient value ($R=0.927$) and statistical significance $>99.9\%$ ($F_{2,9}=27.636$; $F_{2,9\alpha:0.001}=19.9$) and R^2 cross-validated=0.829 indicated it to be a robust model. In order to check the validity and robustness of these models, they were used to predict the activity of partially racemic acids (Table 7), which were not used in deriving these models because of the non-availability of the chiral acids for evaluation. There has been a good correlation between the observed activity of the partially racemized (*S* and *R*) and racemic acids and the predicted activity for chiral *S* and *R* acids (Table 7) and in general the order of activity was chiral *S* $>$ partially racemized *S* $>$ racemic $>$ partially racemized *R* $>$ chiral *R*. Such an agreement between the observed and predicted activities of the partially racemized (*S* and *R*) and racemic acids clearly points towards the predictive comparability of these models, which may be useful for designing modulators which can potentiate anti-nociceptive activity.

In summary, the semi-rigid chiral analogues of *benzotript* have shown potent potentiation of anti-nociception comparable to *benzotript* suggesting that the conformations corresponding to the semi-rigid analogue have major contribution for the activity. The biophore models with three sites corresponding to ring centers of the phenyl and pyrrole ring, nitrogen atom of the pyrrole and pyridine, oxygen atom of the amide or ester and their hydrogen bonding sites (π -electrons) indicate that the three sites A, B and C; the first is A represented by

the phenyl ring of indole part in terms of its 6π electrons presence which are possibly involved in π - π interactions, the second site B being the amidic oxygen in terms of π population, charge and the electron of its lone pair for electrostatic as well as ionic density index and the third site C for the hydrogen bonding. All these sites are important and are involved in the potentiation of anti-nociceptive activity possibly through CCK-B receptor as similar sites, namely a hydrogen bonding site between the carbonyl oxygen of the ligand and properly oriented receptor donor function and in π -rich hydrophobic site between an aromatic π region (indole/phenyl ring) of the ligand in the receptor cavity for hydrophobic interactions have also been suggested for the binding of CCK-B antagonist with the CCK-B receptor. Further, the derived QSAR models not only explain the data for the chiral ester molecules (**3a–3k**; training set compounds, Table 6) used in deriving these models but also explains the observed antinociceptive activity of the partially racemic acids (**4a–4k**; test set compounds, Table 7) and thus can advantageously be explored in the designing of new leads.

Experimental

All chemicals used were of reagent grade unless stated otherwise. Solvents and substituted benzoyl chlorides were distilled prior to use according to standard methods. In high performance liquid chromatography (HPLC) run solvents were used directly from HPLC grade OmniSolv[®] sure seal bottles. Melting points were determined in open capillaries on an electrically heated melting point apparatus and are otherwise uncorrected. Thin layer chromatography (TLC) was run on self-made plates of silica gel G (Acme Synthetic Chemicals, India) or 0.25 mm ready made plates of silica gel 60F₂₅₄ (Kieselgel 60F₂₅₄, E. Merck, Darmstadt, Germany) and detection was done by iodine vapors/spraying with Dragon droff spray reagent or by UV radiation. Column chromatography was performed with silica gel (Acme Synthetic Chemicals, India; 60–120 mesh). Proton nuclear magnetic resonance spectra (¹H NMR) were recorded on Bruker AVANCE DPX 200 MHz or DRX 300 MHz or 400 MHz FT NMR spectrometer at room temperature using CDCl₃ or DMSO-*d*₆ as the solvent. Proton chemical shifts (δ) are reported in parts per million (ppm) relative to tetra methyl silane (TMS, 0.00 ppm). Coupling constants (*J*) are reported in hertz (Hz), and s, d, t, q, m, br, and ex refer to singlet, doublet, triplet, quartet, multiplet, broad, and exchangeable, respectively. Maj and min refers to major and minor conformations, respectively. Infra-red spectra (IR) were recorded on Perkin-Elmer infrared models 557, 881, or Shimadzu FTIR model PC spectrophotometer (ν_{max} in cm⁻¹). Electron impact mass spectra (EIMS) were recorded on Jeol-JMSD-300 spectrometer. Microanalysis (C, H, N) were performed on a Carlo erba instruments CHNS-O EA1108-Elemental Analyzer and results were within 0.4% of the theoretical values unless stated otherwise. Optical rotations were determined on Autopol III Automatic polarimeter using the sodium D-line (c in g/100 mL). NMR, IR, EIMS, microanalyses

and optical rotations were performed at the Regional Sophisticated Instrument Center (RSIC) and chiral HPLC was performed on an analytical Lachrom Merck, Hitachi system at the Medicinal Chemistry Division, Central Drug Research Institute, Lucknow, India. The column used was LiChroCART[®] 250-4 ChiraDex[®] (244×4 mm) of Merck, with an L-7455 Diode Array Detector set for 200–400 nm range, using MeOH/H₂O (30/70) solvent system with flow rate set at 0.8 mL/min having a pressure of 174 psi at 20 °C.

Synthesis of *S*(–)-methyl-1,2,3,4-tetrahydro-9H-pyrido(3,4-b)indole-3-carboxylate (**2a**)

Formaldehyde (38 wt% solution in water, 11 mL) was added to a solution of L-tryptophan methyl ester hydrochloride **1a** (22 g, 0.86 mol) in aq methanol (154 mL; ratio 10:1) during 30 min. The reaction mixture was stirred for 4 h at room temperature, concentrated and cooled to give *S*(–)-methyl-1,2,3,4-tetrahydro-9H-pyrido(3,4-b)indole-3-carboxylate hydrochloride which was basified with sodium bicarbonate to give **2a**. Yield 11.4 g (57%); M.P. 165 °C; $[\alpha]_{\text{D}}^{20}$ –71.00° (*c* 0.6, MeOH); ¹H NMR (200 MHz, CDCl₃): δ 2.83–2.96 (m, 1H, CH₂), 3.16 (dd, *J*=4.64 and 15.28, 1H, CH₂), 3.80 (s, 4H, OCH₃ and CH), 4.13 (bs, 2H, NCH₂), 7.06–7.19 (m, 2H, ArH), 7.30 (d, *J*=7.10, 1H, ArH), 7.47 (d, *J*=8.18, 1H, ArH), 7.83 (brs, 1H, indole NH); FTIR (KBr, cm^{–1}): 738, 820, 866, 1004, 1056, 1128, 1190, 1234, 1302, 1346, 1442, 1504, 1590, 1626, 1740, 1916, 2312, 2752, 2938, 3058, 3150, 3324; MS (EI): *m/z* 230 (M⁺). Anal. calcd for C₁₃H₁₄O₂: C 67.81; H 6.13; N 12.17%. Found: C 67.85; H 6.14; N 12.26%.

Compound *R*(+)-methyl 1,2,3,4-tetrahydro-9H-pyrido(3,4-b) indole-3-carboxylate **2b** was synthesized by the similar method starting from D-tryptophan methyl ester hydrochloride **1b**. Yield 58%; mp 150 °C; $[\alpha]_{\text{D}}^{20}$ +62.84° (*c* 0.5, MeOH); ¹H NMR (200 MHz, CDCl₃): δ 1.75 (bs, 1H, pyrido NH), 2.83–2.96 (m, 1H, CH₂), 3.15 (dd, *J*=4.58 and 15.38, 1H, CH₂), 3.80 (brs, 4H, OCH₃ and CH), 4.12 (brs, 2H, NCH₂), 7.06–7.19 (m, 2H, ArH), 7.30 (d, *J*=7.04, 1H, ArH), 7.48 (d, *J*=7.80, 1H, ArH), 7.85 (brs, 1H, indole NH); FTIR (KBr, cm^{–1}): 724, 802, 1006, 1176, 1256, 1336, 1442, 1738, 1880, 2340, 2848, 2935, 3198, 3726, 3826; MS (EI): *m/z* 230 (M⁺). Anal. calcd for C₁₃H₁₄N₂O₂: C 67.81; H 6.13; N 12.17%. Found: C 67.86; H 6.15; N 12.19%.

Synthesis of *S*(–)-methyl 2-acetyl-1,2,3,4-tetrahydro-9H-pyrido(3,4-b) indole-3-carboxylate (**3l**, R = CH₃)

Acetic anhydride (1.10 mL, 0.011 mol), dry triethylamine (1.60 mL, 0.011 mol) were added to a solution of *S*(–)-methyl-1,2,3,4-tetrahydro-9H-pyrido(3,4-b)indole-3-carboxylate **2a** (2.30 g, 0.01 mol) in dry tetrahydrofuran (THF) (50 mL) and the resulting solution was stirred at room temperature for 4 h. It was then concentrated under reduced pressure and triturated with water to yield crude product (**3l**), which was recrystallized with methanol. Yield = 2.3 g (85%); mp 167–168 °C; $[\alpha]_{\text{D}}^{20}$ +143.64° (*c* 0.22, MeOH); ¹H NMR (300 MHz, CDCl₃) δ 2.26 and 2.27 (s, 3H, COCH₃) 3.06

and 3.47 (dd and d, *J*=6.3, 15.6 and 15.9, 1H, CH₂CHCO₂CH₃), 3.15 and 3.54 (dd and d, *J*=5.76 and 15.6, 1H, CH₂CHCO₂CH₃), 3.59 and 3.62 (s, 3H, OCH₃), 4.73 and 4.84 (d, *J*=15.3 for both, 1H, CH₂N), 4.39 and 5.21 (d, *J*=16.8 and 17.1, 1H, CH₂N), 4.94 and 5.95 (d, *J*=5.7 and 6.2, 1H, CHCO₂CH₃), 7.09–7.20 (m, 2H, Ar-6 and 7-H), 7.26–7.32 (m, 1H, Ar-8-H), 7.51 and 8.63 (t, *J*=4.8, 1H, Ar-5-H), 8.47 (ex, brs, 1H, NH); ¹³C NMR (CDCl₃, 300 MHz) δ 22.0 and 22.1 (C-11), 22.9 and 23.8 (C-4), 39.1 and 42.2 (C-1), 50.5 and 55.9 (C-3), 52.4 and 52.7 (C-13), 104.8 and 106.6 (C-4a), 110.9 and 111.0 (C-8), 117.8 and 118.1 (C-5), 119.4 and 119.6 (C-6), 121.8 and 122.0 (C-7), 126.4 and 126.5 (C-4b), 128.4 and 129.4 (C-9a), 136.4 and 136.5 (C-8a), 170.9 and 171.3 (C-10), 171.5 and 171.6 (C-12); FTIR (KBr, cm^{–1}): 748, 1020, 1188, 1234, 1327, 1435, 1645, 1738, 3217, 3393; MS (EI): *m/z* 272 (M⁺). Anal. calcd for C₁₅H₁₆N₂O₃: C 73.75; H 6.60; N 11.47%. Found: C 73.60; H 6.50; N 11.35%.

Synthesis of *S*(–)-Methyl-2-(4-chlorobenzoyl)-1,2,3,4-tetrahydro-9H-pyrido(3,4-b)indole-3-carboxylate (**3a**, R = C₆H₄-4-Cl)

A mixture of *S*(–)-methyl 1,2,3,4-tetrahydro-9H-pyrido(3,4-b)indole-3-carboxylate **2a** (2.30 g, 0.01 mol), 4-chlorobenzoyl chloride (1.75 g, 0.01 mol) and triethylamine (1.60 mL) in dry THF (50 mL) was refluxed at 90 °C for 8 h. It was concentrated and diluted with H₂O (30 mL). The solid separated was filtered and dried. It was purified by column chromatography on silica gel column using 2% methanol in chloroform as an eluant. Yield 1.9 g (52%); mp 245 °C; $[\alpha]_{\text{D}}^{20}$ –8.25° (*c* 0.21, MeOH); ¹H NMR (400 MHz, CDCl₃): δ 3.10–3.25 (m, 1H, CH₂), 3.40–3.55 (m, 1H, CH₂), 3.65 and 3.70 (s, 3H, OCH₃), 4.55 (d, *J*=16.67, 1H, NCH₂), 4.90 and 5.35 (m, 1H, NCH₂), 4.85 and 6.00 (d, *J*=6.67, 1H, CH), 7.00–7.15 (m, 2H, ArH), 7.25–7.55 (m, 6H, ArH), 9.82 and 10.12 (brs, 1H, indole NH); FTIR (KBr, cm^{–1}): 820, 980, 1080, 1160, 1200, 1280, 1400, 1600, 1720, 2900, 2920, 3060, 3160; MS (EI): *m/z* 368 (M⁺). Anal. calcd for C₂₀H₁₇O₃N₂Cl: C 65.13; H 4.65; N 7.60%. Found: C 65.20; H 4.78; N 7.72%.

Compound *R*(+)-methyl 2-(4-chlorobenzoyl)-1,2,3,4-tetrahydro-9H-pyrido(3,4-b)indole-3-carboxylate **3k**, R = C₆H₄-4-Cl was synthesized by the similar method starting from **2b**. Yield 36%; mp 265 °C; $[\alpha]_{\text{D}}^{20}$ +9.54° (*c* 0.22, MeOH); ¹H NMR (400 MHz, CDCl₃): δ 3.10–3.25 (m, 1H, CH₂), 3.40–3.55 (m, 1H, CH₂), 3.60 and 3.70 (s, 3H, OCH₃), 4.55 (d, *J*=16.67, 1H, NCH₂), 4.80 and 5.35 (d, *J*=16.67, 1H, NCH₂), 5.95 and 4.85 (d, *J*=6.67, 1H, CH), 7.00–7.15 (m, 2H, ArH), 7.25–7.55 (m, 6H, ArH), 10.05 and 10.35 (brs, 1H, indole NH); FTIR (KBr, cm^{–1}): 633, 723, 756, 843, 1015, 1092, 1142, 1173, 1198, 1232, 1421, 1523, 1597, 1632, 1740, 2513, 2750, 2866, 2914, 2955, 3111, 3196; MS (EI): *m/z* 368 (M⁺). Anal. calcd for C₂₀H₁₇O₃N₂Cl: C 65.13; H 4.65; N 7.60%. Found: C 65.22; H 4.79; N 7.75%.

Other compounds (**3b–3j**) were similarly synthesized and their physicochemical data are given in Table 1.

Synthesis of *S*-(–)-2-(4-chlorobenzoyl)-1,2,3,4-tetrahydro-9H-pyrido(3,4-b) indole-3-carboxylic acid (4a, R = C₆H₄-4-Cl)

2 N NaOH (0.6 mL) was added to a stirred solution of *S*-(–)-methyl 2-(4-chlorobenzoyl)-1,2,3,4-tetrahydro-9H-pyrido(3,4-b)indole-3-carboxylate **3a** (0.368 g, 0.001 mol) in methanol or dioxane (10 mL) and the stirring was continued at 25 °C overnight. Reaction mixture was acidified with acetic acid and solution was concentrated to half of its volume and then it was diluted with water (50 mL). The separated solid was filtered, washed with water and dried, purified by passing through silica gel column using 6% methanol in chloroform as eluant. Yield 0.19 g (54%): mp 222 °C; $[\alpha]_D^{20}$ –0.91° (*c* 0.2, DMF); ¹H NMR (400 MHz, DMSO-*d*₆): δ 2.25–2.35 (m, 1H, CH₂), 2.50–2.65 (m, 1H, CH₂), 3.70 (t, *J* = 13.33, 1H, NCH₂), 3.90 and 4.35 (d, *J* = 13.33, 1H, NCH₂), 3.95 and 5.00 (d, *J* = 6.67, 1H, CH), 6.20–6.35 (m, 2H, ArH), 6.45–6.90 (m, 6H, ArH), 9.90 and 10.20 (brs, 1H, CO₂H); FTIR (KBr, cm^{–1}): 642, 682, 722, 754, 838, 888, 908, 968, 1008, 1092, 1136, 1174, 1212, 1246, 1325, 1404, 1448, 1596, 1628, 1714, 2342, 2866, 2928, 3062, 3336; MS (EI): *m/z* 354 (M⁺). Anal. calcd for C₁₉H₁₅O₃N₂Cl: C 64.32; H 4.26; N 7.90. Found C 64.22; H 4.20; N 7.96.

Compound *R*-(+)-2-(4-chlorobenzoyl)-1,2,3,4-tetrahydro-9H-pyrido(3,4-b)indole-3-carboxylic acid (**4k**, R = C₆H₄-4-Cl) was prepared by the similar method. Yield 76%: mp 231 °C; $[\alpha]_D^{20}$ +2.96° (*c* 0.18, DMF); ¹H

NMR (400 MHz, DMSO-*d*₆): δ 2.25–2.35 (m, 1H, CH₂), 2.50–2.65 (m, 1H, CH₂), 3.70 (t, *J* = 13.33, 1H, NCH₂), 3.90 and 4.35 (d, *J* = 13.33, 1H, NCH₂), 3.95 and 5.00 (d, *J* = 6.67, 1H, CH), 6.20–6.35 (m, 2H, ArH), 6.45–6.90 (m, 6H, ArH), 9.90 and 10.20 (brs, 1H, CO₂H); FTIR (KBr, cm^{–1}): 615, 679, 719, 752, 837, 889, 968, 1007, 1092, 1140, 1173, 1209, 1242, 1319, 1408, 1448, 1522, 1597, 1628, 1713, 2561, 2862, 3329; MS (EI): *m/z* 355(M⁺). Anal. calcd for C₁₉H₁₅O₃N₂Cl: C 64.32; H 4.26; N 7.98%. Found: C 64.28; H 4.22; N 7.86%.

Other compounds (**4l**, **4b–4j**) were synthesized by adopting above procedure and their characterization data is given in Table 1.

Assessment of antinociceptive activity

The antinociceptive activity of morphine plus test compound and morphine alone was determined by hot plate test.³⁸ Mice of either sex (18–23 g) bred at the National Laboratory Animal Center of the Institute were used in the group of 10 mice each. The nociceptive response (reaction time, RT) of each animal was monitored on electrically heated and thermostatically controlled hot plate, maintained at 56 ± 0.5 °C. Two pre-drug (base line) reaction times were observed 15 min apart, and the control reaction times varied from 2.5 to 3.5 s. First, graded doses of morphine were administered and percent analgesia was determined at each dose level and ED₅₀ calculated by probit analysis.³⁹ Subsequently various doses of test compound and morphine (ED₅₀ dose)

Table 3. Potentiation of morphine antinociception

Compound	Index of antinociception		Change (C = B–A)	Log (C × 100)
	Morphine (A)	Morphine + compound = (B)		
3a	0.325 ± 0.028	0.491 ± 0.068	0.166	1.220
3b	0.283 ± 0.053	0.400 ± 0.104	0.117	1.068
3c	0.305 ± 0.062	0.395 ± 0.073	0.090	0.982
3d	0.259 ± 0.047	0.338 ± 0.082	0.079	0.898
3e	0.287 ± 0.027	0.459 ± 0.060	0.172	1.235
3f	0.285 ± 0.018	0.376 ± 0.047	0.091	0.959
3g	0.279 ± 0.038	0.449 ± 0.055	0.170	1.230
3h	0.305 ± 0.026	0.600 ± 0.064	0.295	1.469
3i	0.306 ± 0.053	0.468 ± 0.066	0.162	1.209
3j	0.259 ± 0.013	0.305 ± 0.036	0.046	0.663
3k	0.243 ± 0.013	0.279 ± 0.045	0.036	0.556
4a	0.389 ± 0.075	0.559 ± 0.060	0.170	1.230
4b	0.382 ± 0.075	0.554 ± 0.088	0.172	1.235
4c	0.302 ± 0.044	0.415 ± 0.077	0.113	1.053
4d	0.259 ± 0.045	0.290 ± 0.027	0.031	0.491
4e	0.343 ± 0.060	0.365 ± 0.076	0.022	0.342
4f	0.308 ± 0.043	0.407 ± 0.064	0.099	0.996
4g	0.271 ± 0.034	0.340 ± 0.073	0.069	0.839
4h	0.349 ± 0.056	0.609 ± 0.121	0.260	1.415
4i	0.306 ± 0.036	0.380 ± 0.056	0.074	0.869
4j	0.243 ± 0.013	0.328 ± 0.056	0.085	0.929
4k	0.237 ± 0.013	0.288 ± 0.037	0.051	0.700
5a	0.348 ± 0.080	0.514 ± 0.089	0.166	1.220
5b	0.541 ± 0.103	0.721 ± 0.066	0.180	1.255
5c	0.305 ± 0.044	0.463 ± 0.066	0.158	1.198
5d	0.394 ± 0.045	0.452 ± 0.067	0.058	0.763
5e	0.359 ± 0.049	0.624 ± 0.079	0.265	1.423
<i>Benzotript</i>	0.338 ± 0.055	0.619 ± 0.086	0.231	1.363
<i>Proglumide</i>	0.369 ± 0.062	0.571 ± 0.076	0.202	1.305

were co-administered and anti-nociceptive response was measured at 15 min intervals till it reached the basal level. The control group of mice received an equivalent amount of vehicle. Morphine served as control and naltrexone, an opioid antagonist, was used to check the specificity of opioid antinociceptive activity. *Proglumide* and *benzotript* were used as standard.

The data of each group of animals were averaged and converted to an 'index of antinociception'⁴⁰ according to the formula:

Index of Antinociception (IA)

$$= \frac{\text{Test reaction time (TRT)} - \text{Control RT}}{10 - \text{Control RT}}$$

The control RT is the mean of the two basal readings taken at 15 min intervals and a cut-off time of 10 s was used in these experiments to avoid any damage to paw. IA values of 1.0 indicate 100 percent antinociception and IA values of 0 indicate no change in basal RT. The significant increase in IA in compound-treated animals as compared to morphine alone was taken as potentiation of morphine anti-nociception by the test compound (Table 3).

Building up of the molecular model

The molecular structure of the compounds (**3a–3k**, **4a–4k**, *benzotript* and *proglumide*) were constructed on Silicon graphics INDY R-4000 workstation using the sketch program in the Builder Module of INSIGHT II software from the Molecular Simulation Incorporation (MSI).²⁹ The compounds were optimized for their geometry (net charge 0.00 kcal/mol) by setting the forcefield potential action, partial charge action and formal charge action as fixed. The energy minimization method for each compound employed the steepest descent, conjugate gradients and Newton–Raphson's algorithms in sequence followed by Quasi-Newton optimized procedure with a maximum number of iteration set at 1000 and using energy tolerance value of 0.001 kcal/mol. The molecular structures were stored in MDL format and used for the calculation of MOPAC 6.0 (MNDO Hamiltonian⁴¹)-based indices, including atomic charges, π population, and electron donor and acceptor indices. The biophores (pharmacophores) were built with the

APEX-3D module of the molecular simulations software²⁹ on the set of total 13 compounds (Table 5). The overall match quality calculation⁴² is based on all pairwise molecular similarities according to:

$$\text{Match} = \frac{2}{n(n-1)} \sum_{i=1}^n \sum_{j=1+1}^n \frac{\text{Mol sim}(i, j)}{\text{Mol sim}(i, i) + \text{Mol sim}(j, j) - \text{Mol sim}(i, j)} \quad (2)$$

where n is the number of compounds and the Mol sim(i, j) function is calculated according to

$$\text{Mol sim}(i, j) = \sum_{\alpha_i=1}^m \sum_{\alpha_j=1}^n \frac{\text{At sim}(\alpha_i, \alpha_j)}{W_{3D}(\alpha_i, \alpha_j) \times W_{2D}(\alpha_i, \alpha_j)}$$

where n is the number of atoms in molecule I , m is the number of atoms in molecule j , At sim(α_i, α_j) is a function that calculates the similarity of atoms α_i and α_j ,

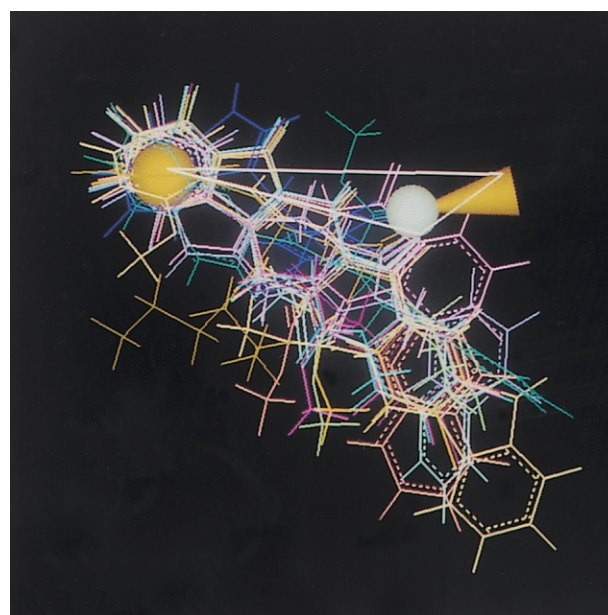


Figure 2. Superimposition of the compounds (**3a–3k**, *benzotript* and *proglumide*) in model no. 1; biophoric sites represented by white/yellow solid spheres and cone: a biophoric pattern for anti-nociceptive activity.

Table 4. 3D-QSAR Models (1–6) describing correlation and statistical reliability for antinociceptive activity

Model	RMSA ^a	RMSA ^b	R ²	Chance	Size	Match	Var. ^c	Comp.
1	0.14	0.15	0.78	0.00	3	0.26	2	13
2	0.11	0.14	0.86	0.01	3	0.39	2	12
3	0.11	0.14	0.86	0.01	3	0.51	2	12
4	0.11	0.14	0.86	0.01	3	0.49	2	12
5	0.11	0.14	0.86	0.00	3	0.45	2	12
6	0.11	0.14	0.86	0.02	3	0.44	2	12

^aRMSA, root mean square error of approximation.

^bRMSP, root mean square error of leave-one-out prediction.

^cVar., variable.

Table 5. Apex-3D Statistical Parameters for the selected six best models

Model	R^2	RMSA	RMSP	F	n	Total hydrophobicity ^a	I^b
1	0.775	0.140	0.152	17.224	13	0.255	-0.628
2–6	0.860	0.113	0.144	27.636	12	0.333	-0.617

^aTotal hydrophobicity, calculated as logP (sum of atomic increments).⁴²

Table 6. Experimental, calculated and predicted activity data and parameter values for the chiral title esters from Apex-3D model no. 1

Compound	Total hydrophobicity ^a	Experimental	Calculated	Calculated error	Predicted	Predicted error
3a	3.10	1.22	1.24	-0.02	1.25	-0.03
3b	3.05	1.07	1.23	-0.16	1.25	-0.18
3c	2.60	0.98	1.12	-0.13	1.13	-0.15
3d	1.85	0.90	0.92	-0.03	0.96	-0.06
3e	2.70	1.24	1.14	0.09	1.13	0.10
3f	2.75	0.96	1.15	-0.20	1.17	-0.22
3g	3.05	1.23	1.23	0.00	1.23	0.00
3h	3.35	1.47	1.31	0.16	1.26	0.21
3i	3.10	1.21	1.24	-0.03	1.25	-0.04
3j	3.05	0.66	0.60	0.06	0.54	0.12
3k	3.10	0.56	0.62	-0.06	0.68	-0.12
<i>Benzotript</i>	3.30	1.36	1.29	0.07	1.28	0.09
<i>Proglumide</i>	2.35	1.30	1.05	0.25	0.99	0.32

^aThe other parameter I, Indicator has value of 1.00 for **3j** and **3k** (*R* config.) and 0.00 for rest compounds (**3a–3i**) (*S* config.) of the series.

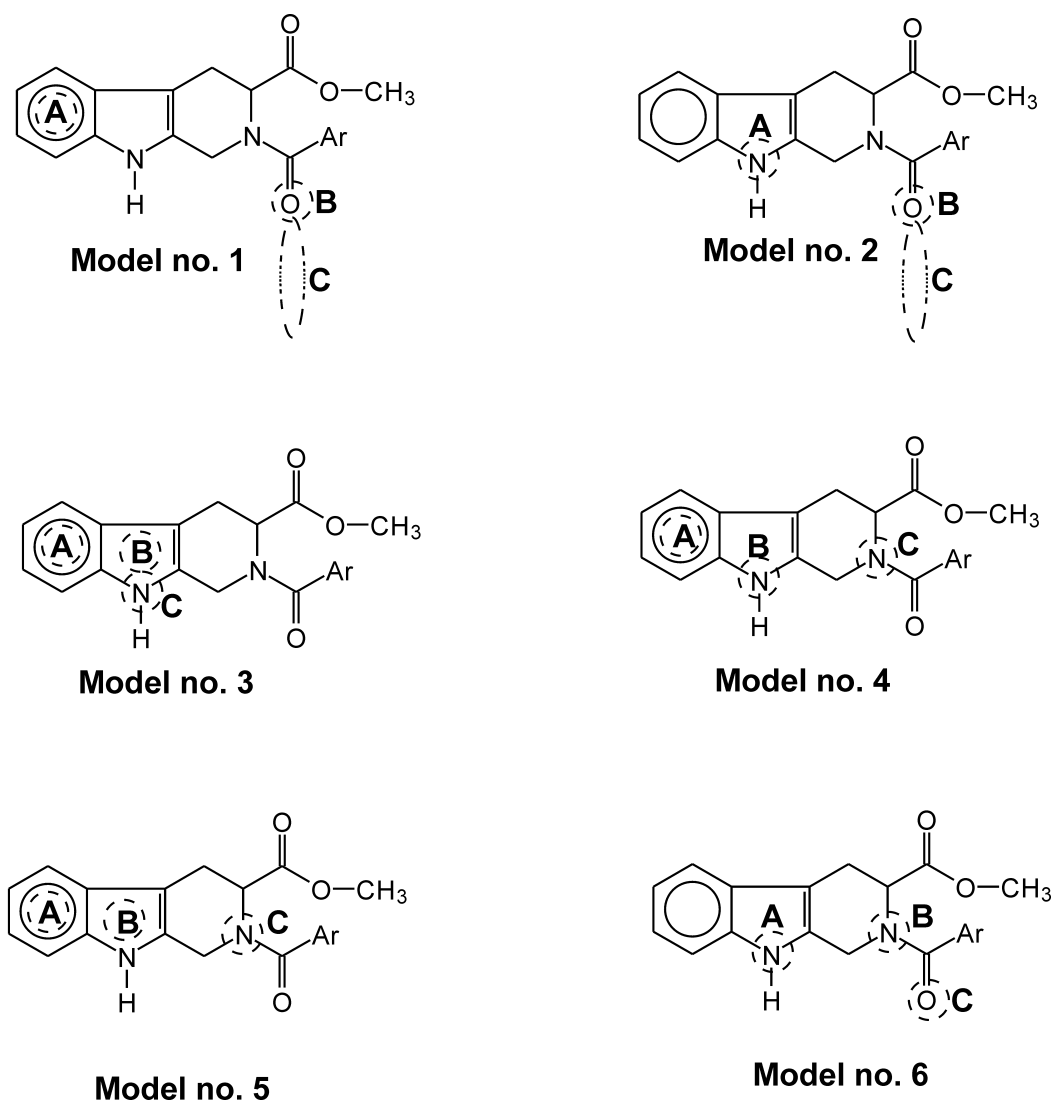
**Figure 3.** Biophoric sites (A, B and C) represented by dotted circles (○) and ovals (◌) on the chiral title esters (**3a–3k**) of model nos 1–6.

Table 7. Comparative data of experimentally observed and calculated biological activity of partially racemized title acids from Apex-3D models

Compound	Experimental	Model no. 1	Model no. 2	Model nos. 3–6
4a	1.23	1.23	—	1.22
4b	1.235	1.22	1.20	1.20
4c	1.053	1.10	1.05	1.05
4d	0.491	0.92	0.82	0.82
4e	0.342	1.13	1.09	1.09
4f	0.996	1.14	1.10	1.10
4g	0.839	1.22	1.20	1.20
4h	1.415	1.31	1.32	1.32
4i	0.869	1.23	1.22	1.22
4j	0.920	0.59	0.58	0.56
4k	0.70	0.60	0.60	0.60

$W_{3D}(\alpha_i, \alpha_j)$ is weighing function for matching atoms based on the Cartesian distances between them, and $W_{2D}(\alpha_i, \alpha_j)$ is a weighting function based on the topological distances of atoms from the biophore.

The 3D-QSAR equations were derived with the site radius set at 0.60, the occupancy at 8, the sensitivity at 0.80, and the randomization at 100. The total hydrophobicity, total refractivity and indicator were selected as global properties. The biophoric centers and secondary sites combined to global properties (total hydrophobicity, total refractivity, and indicator) were used to obtain an equation to predict the percent potentiation of morphine antinociception. The biophoric centers were set to charges, π population, HOMO, LUMO, hydrogen acceptor, hydrogen donor, refractivity and hydrophobicity. The secondary sites were set to hydrogen acceptor, presence; hydrogen donor, presence; heteroatom, presence; hydrophobic, hydrophobicity; steric, refractivity; ring, presence.

Determination of enantiomeric excess (ee)

Enantiomeric excess (ee) was determined for each title compound and was found to be greater than 95% for each chiral title esters (3a–3l) and was assessed in the following manner. Using chiral HPLC analysis (Chiradex[®] column) eluting with isocratic mixture of MeOH/H₂O (30/70), all the chiral esters appeared as a single distinct peak. However, for the partially racemic title acids (4a–4l), baseline separation could not be obtained due to tailing. Several solutions of each synthesized (*R/S* enantiomer) chiral title esters were prepared (2.0 mg/5.0 mL of methyl alcohol) and mixed in the following proportions (95:5, 97.5:2.5 and 98.75:1.25). These solutions were analyzed, and it was found that each enantiomer could easily be detected as a shoulder in the 97.5:2.5 mixture but not in the 98.75:1.25 mixture, which implied that the ee of each of these chiral title esters was at a minimum >95%.

NMR experiment

All experiments were carried out on Bruker AVANCE DRX 300 MHz FT NMR spectrometer equipped with a

5 mm multinuclear inverse probehead with Z-shielded gradient at room temperature using CDCl₃ as a solvent.

300 MHz ¹H, ¹H COSY. relaxation delay $d_1 = 2$ s; 90° pulse, 6.88 μ s for ¹H; 1 k points in t_2 ; spectral width, 8 ppm in both dimension; 256 experiments in t_1 ; linear prediction to 512 points; zero filling up to 1 k and apodization with sine bell in both dimension prior to double Fourier transform.

300 MHz ¹H, ¹H ROESY. relaxation delay $d_1 = 2$ s; 90° pulse, 6.88 μ s for ¹H; spin lock = 250 μ s; 1 k points in t_2 ; spectral width 8 ppm in both dimension; 256 experiments in t_1 ; linear prediction to 512 points; zero filling up to 1 k and apodization with 90° shifted sine bell in both dimension prior to double Fourier transform.

Acknowledgements

The authors are thankful to Dr. Raja Roy and Mr. B.S. Joshi for the NMR studies, Mr. A.S. Kushwaha for the technical assistance in molecular modeling and QSAR and SKP is grateful to CSIR, New Delhi for a senior research fellowship.

References

- Portnoy, R. K. In *Proceedings of the 7th World Congress on Pain, Progress in Pain Research and Management*; Crebhart, G. F., Hammond, D.L., Jensen, T. S. Eds. IASP, Seattle, WA, 1994; Vol. 2, pp 595–619.
- Foley, K. M. Clinical Tolerance to Opioids: In *Towards a New Pharmacotherapy of Pain*; Basbaum, A. I.; Besson, J. M. Eds. John Wiley & Sons Ltd. New York, 1991; pp 181–203.
- Herman, B. H.; Vocci, F.; Bridge, P. *Neuropsychopharmacology* **1995**, *13*, 269.
- Kolesnikov, Y. A.; Pick, C. G.; Pasternak, G. W. *Eur. J. Pharmacol.* **1992**, *221*, 399.
- Trujillo, K. A.; Akil, H. *Science* **1991**, *251*, 85.
- Trujillo, K. A.; Akil, H. *Brain Res.* **1994**, *633*, 178.
- Trujillo, K. A.; Akil, H. *Drug Alcohol Depend.* **1995**, *38*, 139.
- Arends, R. H.; Hayashi, T. G.; Luger, T. J.; Shen, D. D. *JPET* **1998**, *286*, 585.
- Hui, S. G.; Sevilla, E. L.; Ogle, C. W. *Br. J. Pharmacol.* **1996**, *118*, 1044.
- Zarrindast, M. R.; Sajedian, M.; Rezayat, M.; Ghazi-Khansari, M. *Eur. J. Pharmacol.* **1995**, *273*, 203.
- Basbaum, A. I.; Fields, H. L. *Ann. Rev. Neurosci.* **1984**, *7*, 309.
- Fields, H. L.; Heinrich, M. M.; Mason, P. *Ann. Rev. Neurosci.* **1991**, *14*, 219.
- Le Bars, D. In *Neuronal Serotonin* Osborne, N. N., Hamon, M. Eds.; John Wiley & Sons Ltd. New York, 1988; pp 171–228.
- Watkins, L. R.; Kinscheck, I. B.; Mayer, D. J. *Science* **1984**, *224*, 395.
- Fairs, P. L.; Komisaruk, B. R.; Watkins, L. R.; Mayer, D. J. *Science* **1983**, *219*, 310.
- Wank, S. A.; Pisegna, J. R.; DeWeerth, A. *Proc. Natl. Acad. Sci. U.S.A.* **1992**, *89*, 8691.
- Lee, Y.-M.; Beinborn, M.; McBride, E. W.; Lu, M.; Kolakowski, L. F., Jr.; Kopin, A. S. *J. Biol. Chem.* **1993**, *268*, 8164.

18. DeWeerth, A.; Pisegna, J. R.; Huppi, K.; Wank, S. A. *Biochem. Biophys. Res. Commun.* **1993**, *194*, 811.
19. Wank, S. A.; Pisegna, J. R.; DeWeerth, A. *Ann. N. Y. Acad. Sci.* **1994**, *713*, 49.
20. Beinfeld, M. C. *Neuropeptides* **1983**, *3*, 411.
21. Kopin, A. S.; Lee, Y. M.; McBride, E. W.; Miller, L. J.; Lu, M.; Lin, H. Y.; Kolakowski, L. F., Jr.; Beinborn, M. *Proc. Natl. Acad. Sci. USA.* **1992**, *89*, 3605.
22. Pisegna, J. R.; DeWeerth, A.; Huppi, K.; Wank, S. A. *Biochem. Biophys. Res. Commun.* **1992**, *189*, 296.
23. Lindfors, N.; Linden, A.; Brene, S.; Sedvall, G.; Persson, H. *Prog. Neurobiol.* **1993**, *40*, 671.
24. Altar, C. A.; Boyar, W. C. *Brain Res.* **1989**, *483*, 321.
25. Singh, L.; Lewis, A. S.; Field, M. J.; Hughes, J.; Woodruff, G. N. *Proc. Natl. Acad. Sci. USA.* **1991**, *88*, 1130.
26. Bradwejn, J. In *Cholecystokinin Anxiety: Neuron Behavior*; Bradwejn, J., Vasar, E., Eds.; Landes: Austin, TX, 1995; pp 73–86.
27. Hahne, W. F.; Jensen, R. T.; Lemp, G. F.; Gardner, J. D. *Proc. Natl. Acad. Sci. USA.* **1981**, *78*, 6304.
28. Tripathi, R. C.; Patnaik, G. K.; Saxena, A. K. *Indian J. Chem.* **1989**, *28B*, 333.
29. *InsightII*, version 2.3.0; Biosym Technologies: San Diego, 1993.
30. Kubinyi, H., Ed. *3D QSAR in Drug Design. Theory, Methods, and Applications*; ESCOM Science: Leiden, 1993.
31. Crippen, G. M. *J. Comput. Phys.* **1977**, *24*, 96.
32. Viswanadhan, V. N.; Ghose, A. K.; Weinstein, J. N. *Biochem. Biophys. Acta* **1990**, *1039*, 356.
33. Viswanadhan, V. N.; Ghose, A. K.; Hanna, N. B.; Matsumoto, S. S.; Avery, T. L.; Revankar, G. R.; Robins, R. K. *J. Med. Chem.* **1991**, *34*, 526.
34. Saxena, A. K.; Saxena, M.; Chi, H.; Weise, M. *Med. Chem. Res.* **1993**, *3*, 201.
35. Golender, V. E.; Rozenblit, A. B. In *Logical and Combinatorial Algorithms for Drug Design*; Research Studies: UK, 1983.
36. Saxena, A. K.; Jain, P. C.; Anand, N.; Dua, P. R. *J. Med. Chem.* **1973**, *16*, 560.
37. Greco, G.; Novellino, E.; Silipo, C.; Vittoria, A. *Proceedings of the 9th European symposium on Structure Activity Relationships: QSAR and Molecular Modelling*; Wermuth, C. G., Ed.; ESCOM: Leiden, 1993; pp 466–470.
38. Eddy, N. B.; Leimbach, D. *J. Pharmacol. Exp. Ther.* **1953**, *107*, 385.
39. Finney, D. J. In *Probit Analysis*. Cambridge University Press, Cambridge, UK, 1971.
40. Azami, J.; Llewelyn, M. B.; Roberts, M. H. T. *Pain* **1982**, *12*, 229.
41. Dewar, M. J. S.; Thiel, W. *J. Amer. Chem. Soc.* **1977**, *99*, 4899, 4907.
42. *Apex-3D User Guide*; Biosym/MSI: San Diego, 1993.